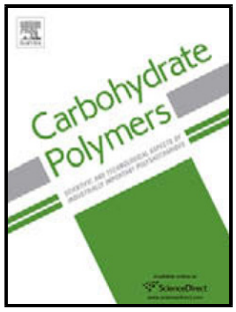

Title: Dielectric and electric properties of new chitosan-hydroxyapatite materials for biomedical application: dielectric spectroscopy and corona treatment

Author: Ivo Petrov Oksana Kalinkevich Maksym Pogorielov Aleksei Kalinkevich Aleksandr Stanislavov Anatoly Sklyar Sergei Danilchenko Temenuzhka Yovcheva

PII: S0144-8617(16)30654-3
DOI: http://dx.doi.org/doi:10.1016/j.carbpol.2016.05.110
Reference: CARP 11179

To appear in:

Received date: 5-2-2016
Revised date: 11-5-2016
Accepted date: 29-5-2016

Please cite this article as: Petrov, Ivo., Kalinkevich, Oksana., Pogorielov, Maksym., Kalinkevich, Aleksei., Stanislavov, Aleksandr., Sklyar, Anatoly., Danilchenko, Sergei., & Yovcheva, Temenuzhka., Dielectric and electric properties of new chitosan-hydroxyapatite materials for biomedical application: dielectric spectroscopy and corona treatment.*Carbohydrate Polymers* http://dx.doi.org/10.1016/j.carbpol.2016.05.110

Dielectric and electric properties of new chitosan-hydroxyapatite materials for biomedical application: dielectric spectroscopy and corona treatment

Ivo Petrov[1,2], Oksana Kalinkevich[3], Maksym Pogorielov[4], Aleksei Kalinkevich[3], Aleksandr Stanislavov[3], Anatoly Sklyar[5], Sergei Danilchenko[3], Temenuzhka Yovcheva[2]

[1]University Hospital "Dr. Georgi Stranski", Pleven, Bulgaria
[2]Department of Experimental Physics, Physics Faculty, University of Plovdiv, Bulgaria
[3]Institute of Applied Physics, Sumy, Ukraine
[4]Sumy State University, Sumy, Ukraine
[5]Sumy State Pedagogical University, Sumy

Highlights

Chitosan-hydroxyapatite do not have intrinsic electret properties

It is not possible to charge them with corona treatment

The ε values of chitosan-hydroxyapatite composites are similar those of bone tissues

Abstract: Chitosan-hydroxyapatite composite materials were synthesized and the possibility to make their surface charged by corona discharge treatment has been evaluated. Dielectric and electric properties of the materials were studied by dielectric spectroscopy, including application of equivalent circuits method and computer simulations. Dielectric spectroscopy shows behavior of the materials quite different from that of both chitosan and HA alone. The obtained dielectric permittivity data are of particular interest in predicting the materials' behavior in electrostimulation after implantation. The ε values observed at physiological temperature in the frequency ranges applied are similar to ε data available for bone tissues.

Keywords: Chitosan; composite; hydroxyapatite; electric properties; dielectric spectroscopy; corona discharge

Introduction

Carbohydrate biopolymers attract attention because of their unique physico-chemical and biological properties. They allow one to create a variety of materials. An important area of their application is medicine: the creation of biologically active agents, materials for drug encapsulation, the preparation of scaffolds for tissue engineering, etc. In this case, it is important that these polymers are non-toxic, biocompatible, and able to provide optimal conditions for adhesion, expansion and cell immobilization thus promoting the integration of an implant with the surrounding tissue. One of the most promising polymers in this respect is chitosan, derived from natural chitin. Chitosan is a product of chitin deacetylation; its macromolecule comprises 2-amino-2-deoxyglucopyranose and 2-acetamido-2-desoxyglucopyranose monomers; their percentage is called the degree of deacetylation of chitosan. Chitosan possesses antioxidant, antibacterial, radioprotective, immunomodulatory properties, fibre- and film-forming ability, it is non-toxic, can be easily modified or used in making composite materials capable of biodegradation. Its electrical characteristics (e.g. volume resistivity and electret properties), poorly studied at present, strongly influence the properties and biological activity of chitosan-based materials.

One of the most effective ways of varying the characteristics of various polymers is to create composites based on them. In this paper, chitosan-based composite materials with nanoscale hydroxyapatite (HA) are studied. HA, the mineral component of bone, is absolutely harmless to a living organism non-toxic polarizable material. HA is a crystalline form of calcium phosphate with either monoclinic or hexagonal crystal symmetry. The stoichiometric formula of HA is $Ca_5(PO_4)_3(OH)$, although the crystal structure can exist in a wide range of nonstoichiometric compositions. The chemical composition of HA can be widely varied by partial substitution by other ions of calcium, phosphate, or hydroxyl at their positions in the crystal lattice. The hydroxyl groups form linear columns along the crystallographic c-axis that give rise to the dielectric properties of HA, including high temperature proton conductivity, ferroelectricity, piezoelectricity, pyroelectricity and electret behavior. Hydroxyapatite is the primary mineral component of bone tissue, and the osteoconductive properties of synthetic HA have led to its widespread use as coating or additive in bone grafts, scaffolds, and orthopedic implants. It has been shown that electrical polarization of HA enhances bioactivity and osseointegration, both *in vitro* and *in vivo*.

Generally, a surface with net positive or negative charge, compared to neutral one, is expected to be more hydrophilic, facilitating interfacial processes and protein adsorption (B. D. Boyan, 1996). Furthermore, surface charge has been shown to increase osteoblast adhesion and early stage bone mineralization at the bone-implant interface with two main mechanisms suggested for surface charge's positive affecting of materials' osseointegration: by forming an apatite layer (adsorbing Ca^{2+} and PO_4^{3-}) and by adsorbing certain types of proteins with desirable reactions with bone-forming cells (Shelton 1991; Guo, 2012). Thus, surface charge modification of bone scaffold materials is a promising new direction for improving their biological properties and performance. Although it is a relatively new approach, it has been rapidly gaining attention, with a lot of research focusing on effective and practical techniques that create a long-lasting electric field on the material surface. All applied methods can be roughly categorized in two main groups: chemical modification of the surfaces, producing charged groups along them with one predominating polarity (Hoven V.P., 2007), and physical methods, producing electret materials - quasi-permanently polarized and having accumulated surface charge of opposite polarity on two opposite sides (Sessler, 1999). One of the physical surface charge modification methods for obtaining electrets is the corona discharge treatment (also known as air plasma treatment) of the materials (T.A. Yovcheva, 2010), a surface modification method that utilizes a low temperature corona discharge plasma, generated at a sharp tip electrode with the application of high voltage, to impart changes in the properties of a surface.

Several works are devoted to the preparation of electret chitosan films and the study of their biological properties. Chitosan electret membranes exhibit stable surface charges, with

good bioactivity and biodegradability. Yanying Wang et al. studied the effects of chitosan bioelectret membrane on bone regeneration in a rabbit cranial defect model. The bioelectret was fabricated by film casting and polarized by grid-controlled corona charging (−1 kV). The bioelectret membrane recipients had a significantly higher volume of newly formed bone and greater rate of material degradation than the non-polarized membrane recipients. Furthermore, the bioelectret membrane induced new bone formation not only around the host bone but also in the center of the defect. Chitosan bioelectret membranes have been shown to have an apparent potential for guided bone regeneration applications. Additionally, some data suggest that chitosan surfaces, that have been chemically modified to be positively or negatively charged, can increase protein adsorption on the material surface, explained in terms of electrostatic attraction and repulsion, and, as a result, mediate cell-scaffold interactions and improve cell adhesion (Hoven V.P., 2007).

There is some data published on dielectric/impedance spectroscopy and related methods of chitosan materials in the form of films. E.I. Bobritskaya et al. investigatad chitosan polymer films by dielectric and thermally activated spectroscopy. The same authors studied chitosan films with a mineral filler by dielectric spectroscopy, showing that the conductivity of the biopolymer decreases with the addition of filler particles. In the work of Atif Islam et al. the effect on conductivity of chitosan-silane crosslinked-poly(vinyl alcohol) blended films due to change in the concentration of PVA and temperature was investigated by impedance spectroscopy and showed good conductance properties. The ionic conductivity of the films initially increased with the increase in temperature for all synthesized samples, which showed an increase in the number of effective charge carriers, and decreased at a specific higher temperature for each film. P. Murugaraj studied the hydration of chitosan films by dielectric spectroscopy in a conventional constraining plate configuration and did comparison with free standing films. In the study of K.S. Zhao et al the dielectric properties of chitosan microsphere beads in aqueous electrolyte solutions were investigated in the 1–500 MHz frequency range. Distinct dielectric relaxation was observed around 10 MHz in weakly acidic solutions (pH 4–6) and the relaxation intensity depended on the electrolyte concentration. Using the relatively nondestructive electrochemical impedance spectroscopy method, that also can be performed under physiologically relevant conditions, some authors were able to obtain data on pore characteristics of chitosan materials comparable to that of scanning electron microscopy (SEM) and mercury intrusion porosimetry (MIP), two commonly used methods for scaffold characterization which require dry samples and vacuum conditions for measurement (Tully-Dartez, 2009).

Much more research has been done on surface charged HA and HA-based materials. Electric and dielectric properties of HA can be influenced significantly by the orientation of OH^- ions in HA crystals. Cong Fu et al. demonstrate that hydroxyapatite retains surprisingly large stored charge when synthesized electrochemically from aqueous solution. Some publications describe the production of surface-charged HA by polarization by proton transport under DC fields in the order of few kV/cm at high temperatures (200-400˚C), where large surface charges can be induced. The surface-charged HA scaffolds have shown a significantly increased osteoblast adhesion, cell proliferation and metabolic activity compared to non-charged controls and performed much better in *in vitro* and *in vivo* tests, accelerating new bone formation (Tarafder, 2011; Bodhak, 2009; Dekhtyar 2008; Itoh, 2006). The study of the electric and dielectric properties of HA, to big extent by dielectric/impedance spectroscopy and related methods, has also been of interest for a number of potential applications, including bone grafts (Gittings, 2009; Zacharov, 2001). Importantly, HA materials exhibit piezoelectric and pyroelectric properties (Gittings, 2009; Tofail, 2009; Baxter, 2009), just as bones do, and which are important in bone growth and remodelling (Telega, 2002; Fukada, 1981). Electric and dielectric properties of HA have also been studied in regard of materials' interaction with electrical fields applied to improve fracture healing and enhance bone growth (Gittings, 2009).

A lot of studies have examined the electrical and dielectric properties of HA and HA-based materials. However, the studies of dielectric characteristics of chitosan/HA composites are

virtually absent. There are only scarce reports about obtaining electret composites. Miho Nakamura et al. evaluated the effects of composite wound dressing films made of silk fibroin (SF) containing hydroxyapatite (HA) or polarized HA (pHA) powders on endothelial cell (EC) behaviors that have important roles in the wound-healing process. In the investigation of Yi Li Qu et al., chitosan/nanoHA electret membranes with negative charges were fabricated by grid-controlled constant voltage corona charging. In this study chitosan/nHA membranes preparation included several stages: synthesis of nanoHA, adding suspension by drops into chitosan solution, ratio nHA/chitosan was 60:40, membranes were crosslinked by glutaraldehyde.

To our knowledge, nor data on investigations on obtaining surface-charged chitosan-HA by physical methods (e.g. by corona discharge method), nor dielectric spectroscopy data for chitosan-HA composite materials have been published.

The aim of the present study was to synthesize and characterize chitosan-HA composite materials; to evaluate the possibility to obtain surface-charged chitosan-HA with corona discharge treatment; to study the materials' dielectric and electric properties by dielectric spectroscopy with analysis of the obtained data, including application of the equivalent circuits method and computer simulations.

Materials and methods

Synthesis of chitosan-HA composite materials

Chitosan (deacetylation degree 82%) was purchased from "Bioprogress" CJSC (Moscow, Russia). The materials were synthesized by coprecipitation method (Danilchenko, 2011) using different concentrations of chitosan solution (6g/l and 10g/l). 1M $CaCl_2$ and 1M NaH_2PO_4 solutions were added to the chitosan solution, pH was slowly increased up to 12 using 5% NaOH solution. The obtained suspension aged for 24 h, and then was rinsed several times with distilled water and dried in a mold during a week to obtain dense samples (Fig. 1). Part of the samples was covered with silver nanolayer on one side (30-50nm Ag) in vacuum chamber VUP-5M (SELMI, Ukraine).

Characterization of the synthesized materials

X-ray diffraction (XRD) crystallographic investigations were performed using DRON4-07 diffractometer ("Burevestnik", Russia). Ni-filtered CuKα radiation (wavelength 0.154nm) was used with a conventional Bragg-Brentano geometry ϑ-2ϑ (where 2ϑ is Bragg's angle). The current and the voltage of the X-ray tube were 20 mA and 30 kV respectively. The samples were measured in the continuous registration mode (at a speed of 2 °/min) within the 2ϑ-angle range from 8° to 60°. All experimental data processing procedures were performed with the program package DIFWIN-1 ("Etalon PTC" Ltd.). Phase identification was performed using JCPDS card catalog (Joint Committee on Powder Diffraction Standards). XRD patterns are shown on Fig. 2. X-Ray phase analysis shows the presence of only phase – hydroxyapatite (JCPDS 9-432) – with poor crystallinity. In sample (b) the overall crystallinity is higher compared to sample (a).

Scanning electron microscopy was performed using the electron microscope REMMA102 (SELMI, Ukraine). The instrument allows visualization of sample surface with the limit resolution of ca. 10 nm. In this work the accelerating voltage of the electron probe was set to 20 kV, the current of the probe was set to 2 nA. To avoid surface charge accumulation in the electron-probe experiment, samples were covered with the thin (30-50 nm) layer of silver in the vacuum set-up VUP-5M (SELMI, Ukraine). As it is seen in Fig. 3, both 6 g/L and 10 g/L composites form dense nonporous material with surface of moderate roughness.

The IR spectra were recorded with the Perkin Elmer Spectrum One spectrometer. During the experiment, all samples individually were ground to powder together with KBr crystals and compressed into tablets.

The bands at 2900, 1665, 1595 and 1543 cm^{-1} are ascribed to methylene ($-CH_2$), amid I, amino ($-NH_2$) and amid II (-NH), correspondingly, in the chitosan (Fig. 5).

The bands at 1031, 963, 603 and 565 am^{-1} correspond to the phosphate group PO_4 in HA, while the band at 3570 cm^{-1} belongs to hydroxyl group OH in HA.

The bands at 1453, 1422 and 875 cm^{-1} are carbonate ions in HA crystals (Yamaguchi I., 2001).

The band at 3600 cm^{-1} is water.

Corona discharge treatment and surface potential measurement

Corona discharge treatment of some of the Chitosan-HA composite samples was carried out in the "Physics of dielectrics" laboratory of the Department of Experimental Physics, University of Plovdiv, by means of a conventional three-electrode system, consisting of grounded plate electrode, corona electrode and a grid placed between them. The three-electrode system was installed in a thermoregulated chamber.

The setup allowed for positive and negative corona treatment for predefined time intervals, at various predefined temperatures (25°C-150°C), applying different voltages and polarities of the corona electrode (U_c) and the grid (U_g), varying the distance between the corona electrode and the grid and the distance between the grid and grounded plate electrode, as well as the removal of the grid from the system.

Samples' surface potential was measured by the method of the vibrating electrode with compensation with estimated error better than ±5% (Reedyk, 1968).

Dielectric spectroscopy

The impedance spectra of samples without Ag covering were measured in the "Physics of dielectrics" laboratory of the Department of Experimental Physics, University of Plovdiv, utilizing a dielectric spectroscopy system, schematically represented in Fig. 5.

Measurement of the impedance characteristics amplitude $|Z|$ and phase φ in the frequency range 20 Hz to 1 MHz is done with the QuadTech Inductance Analyzer 1910 device. The studied sample (2) is placed between two flat parallel electrodes (1), fixed with PTFE holder and a spring. The sample/electrodes system is placed in a thermoisolated chamber (6), allowing for linear heating (0.80°C/min) of the sample by means of a heater (4), connected to a power supply (5). The temperature is measured and monitored by means of a sensor (3), connected to a digital multimeter Agilent 34405A.

Prior to proceeding with the measurements for obtaining the data presented and analysed in this paper we did pilot measurements to check for non-negligible electrode polarization effects using Ag-covered samples, gold electrodes, varying the distance between the electrodes and using samples of different thickness. We did not find any significant difference in the observed spectra, indicating electrode polarization effects, with the different pilot measurements described.

The described dielectric spectroscopy system was used for studying the properties of chitosan-HA samples without Ag covering. As the samples were heated their impedance spectra were obtained at the following temperatures: room temperature 25°C, physiological temperature 37°C, 50°C, 75°C and 100°C. The spectra were recorded on a computer, by means of a serial digital interface and specially modified for the experiment QBasic program, in data format (f, |Z|,

φ), where f is the AC frequency in Hz. The real and imaginary parts of the impedance *Z'* and *Z''* for all frequencies and temperatures were calculated using formulas (1) and (2).

$$Z' = |Z| \cos\varphi \quad (1)$$

$$Z'' = |Z| \sin\varphi \quad (2)$$

The dielectric permittivity ε for all frequencies and temperatures were calculated using formula (3), where $\omega = 2\pi f$ is the angular frequency and C_0 is the so-called "empty cell capacitance". C_0 is calculated using formula (4), where d is the studied sample's thickness, S - the flat parallel electrode surface and $\varepsilon_0 = 8{,}854.10^{-12}\ F/m$ is the permittivity of free space.

$$\varepsilon = \frac{-Z''}{\omega C_0 (Z'^2 + Z''^2)} \quad (3)$$

$$C_0 = \varepsilon_0 \frac{S}{d} \quad (4)$$

The specific conductivity for all frequencies and temperatures were calculated using formula (5).

$$\sigma = \frac{d}{|Z|.S} \quad (5)$$

Further impedance data analysis was done with the software EC-Lab® 10.36 demo (http://www.bio-logic.info/), including regression of equivalent circuits' to experimental data, fitting and simulating the model circuits.

Results and discussion

Corona discharge treatment and surface potential measurement

Ag-covered (nanolayer on one side) chitosan-HA samples were corona treated. 4 days prior to the corona discharge treatment 4 samples were stored in saturated vapor (RH100%), 4 - in dry air (RH0%) and the rest - in room conditions. The samples were placed with the Ag-covered side on the grounded plate electrode. In the series of corona discharge treatments of samples the following parameters were varied: the polarity of the corona electrode and the voltage U_c - in the range (1-10) kV, the polarity of the grid and the voltage U_g - in the range (0-1000) V, as well as situations without grid in place, the time of treatment - (1-10) min, the distance between the grounded plate electrode and the corona electrode - in the range (9-11) mm, the distance between the corona electrode and the grid - (3,0 / 3,5) mm and the temperature (25°C-100°C).

Before and after the corona treatment the surface potential U_s of each sample was measured by the method of the vibrating electrode with compensation. No significant $|Us|>0$ was measured prior to the corona treatment, i.e. there is no evidence of any intristic to the materials surface charge. No significant $|Us|>0$ was also measured in all samples after treatment, i.e. we could not produce chitosan-HA electrets with the applied method of corona discharge treatment in any of the combinations of the varied parameters of the coronating system. There might be success in producing electret samples at temperatures 200°C-400°C, because of the expected polarization of the HA nanocrystals, but such high temperatures are not applicable in the case of chitosan-HA composites, because of the chitosan degradation and inevitable significant change in the biological properties and behavior of the materials.

The connection of HA with chitosan may probably decrease conductivity, and interaction with chitosan could cause different configuration of OH groups. The temperature may be not high enough to polarize HA.

Dielectric spectroscopy results

Nyquist plots $Z''(Z')$, Bode plots $Z(f)=|Z|(f)$ and $\varphi(f)$, the frequency dependence of the dielectric permittivity $\varepsilon(f)$ and specific conductivity $\sigma(f)$, as well as the temperature dependence of the impedance modulus $|Z|(T)$ at low frequency (20Hz) were measured for chitosan-HA samples, prepared with 10g/l chitosan solution and with 6g/l chitosan solution.

Data analysis, equivalent circuits and computer simulations.

The dielectric spectroscopy data, obtained for chitosan-HA samples, prepared with 10g/l chitosan solution, and for those, prepared with 6g/l chitosan solution, show identical behavior of the materials, with no notable differences appearing in the further data interpretation and analysis, and, thus, we discuss them together.

For all samples at all temperatures there we observed decreasing of the impedance modulus Z, increasing of the specific conductivity σ and increasing of the dielectric permittivity ε (Fig. 7) with the increasing of the frequency f, a typical dielectric behavior.

We observed specific frequency domain behavior of the phase shift φ (Fig. 6). While φ remains negative in the whole studied frequency range, its magnitude initially decreases with the frequency, reaching a peak (minimum magnitude), after which its magnitude increases again with the frequency. The peak is observed at different frequencies for the different temperatures and its position shows specific temperature dependence - with the increasing of the temperature T from 25°C to 75°C we observe shifting to higher frequencies and for the temperatures above (100°C) - abrupt shift back to the lower frequencies.

With the increasing of the temperature T from 25°C to 75°C we observed decreasing of Z and increasing of the specific conductivity σ and dielectric permittivity ε (Fig. 7) at all frequencies. Above 75°C we observed abrupt change in the materials' behavior from that trend with increasing of Z and decreasing of σ and ε with the temperature, with all the plots for 100°C being quite similar to those for 50°C. Graphically represented also is the temperature dependence of the impedance modulus Z for the lowest studied frequency (20Hz) (Fig. 8), showing the characteristic peak minimum around 75°C.

The observed abrupt changes in the material's behavior at higher temperatures we attribute to the expected chitosan degradation at around 70°C-80°C. Chitosan degradadion leads to irreversible changes in and loss of some of the important biological properties of the material. Dielectric spectroscopy could be used as non-destructive method for evaluation of chitosan preservation/stability and, respectively, the material's properties during storage under different conditions and after different treatments, e.g. different sterilization methods.

The obtained data for the dielectric permittivity ε (Fig. 7) are of particular interest considering the materials' behavior in electrostimulation after implantation and the ε values observed at physiological temperature in the frequency ranges applied in such procedures are in the order of magnitude of reported measurements of the dielectric permittivity of bone tissues (Ckakkalakal, 1980).

Nyquists plots in all cases show dominant close to linear relationship between the real Z' and imaginary Z'' parts of the impedance, appearing as diagonals inclined at an angle of approximately 45° (slope -0.5). Such behavior is typical for and suggests modeling with equivalent circuits containing Warburg element. φ's shifts towards larger values than that of an ideal Warburg impedance (Fig. 6) indicate additional capacitive behavior. Following on these observations and to further interpret the dielectric spectroscopy results we worked on different equivalent circuits, regressing them, fitting them to the experimental data to estimate the circuit elements' parameters and each circuit's adequacy as a model of the material's behavior. We worked with experimental data obtained at physiological temperature for chitosan-HA 50/50, prepared with 10g/l chitosan solution. In this paper we present our results for two such

equivalent circuits. Model 1 (Fig. 9) is the so-called Randle's modified circuit, a frequently used in similar situations equivalent circuit, and Model 2 (Fig. 10) is a suggested by us equivalent circuit that we have found to best model the material's behavior within the studied frequency range. It should be noted that, although the Warburg distributed element is widely used in electrochemical impedance spectroscopy for modeling impedance due to diffusion, here its appearance in the model circuit is not attributed to any diffusion taking place. Instead, in our case, the Warburg element directly represents a mathematically equivalent to it distributed RC transmission line. Such "transmission line" behavior can be expected in complex heterogeneous materials, composites, materials that have numerous microphases and/or microlayers throughout, as well as with porosity.

It should also be noted that both models are empirical and arbitrary, i.e. circuit components are mostly chosen to give the best possible match between the model and the experimental data. While physical models, where each of the circuit's components is postulated to represent a physical process taking place, (e.g. polarization mechanism) are generally preferable to empirical models, a non-arbitrary physical model choice is mostly possible only for not so complex materials. To come up with such a non-arbitrary physical model circuit for the studied chitosan-hydroxyapatite composite is largely impossible. While we can agree that interfacial polarization of the phase interface is much larger than the polarization induced by ion conduction and also interpret the R and C elements of the Warburg „transmission line" as implying polarization, induced by ion conduction, and interfacial polarization, correspondingly, and the capacitors as implying bulk polarization / interfacial polarization, we fall short of fully addressing the relations between dielectric data and experimental frequency, i.e. the polarization mechanism. Our analysis and conclusions presented in current paper are in no way against proper analysis of polarization mechanism, which problem, we believe, should addressed in a dedicated study and with different approaches.

Fig. 9, 10 come from the EC-Lab® 10.36 demo output and each of them presents the evaluated equivalent circuit (a), its parameters (b) and Nyquist (c) and Bode (d) plots of the the experimental data and the simulated model circuit. Both models show good fit in *Z''(Z')* and *Z(f)*, but the fit is much better with Model 2. Model 1 looks inadequate when we look at *φ(f),* while with Model 2 we have very good fit of the simulated Bode plot *φ(f)* with the experimental data, showing that the model is also accounting for trend for the phase angle to increase in the lowest and highest frequencies of the studied range (under 20 Hz and above 1 MHz).

Conclusion

Chitosan-HA composites prepared by one-step coprecipitation method do not have intrinsic electret properties and it is not possible to achieve such with corona treatment, i.e. to obtain chitosan-HA corona electrets in the temperature range 25°C-100°C. Successful charging might occur with treatment at 200°C-400°C, due to the expected polarization of HA nanocrystals, but such high temperatures are unapplicable, because of the inevitable degradation of chitosan, leading to loss of important biological properties of the composite material. Dielectric spectroscopy results show behavior of the materials quite different from that of both chitosan and HA alone. Suggested is a simplified equivalent circuit with a Warburg element (representing a distributed RC transmission line) that models materials' behavior within the studied frequency range very well. The obtained dielectric permittivity data are of particular interest in predicting the materials' behavior in electrostimulation after implantation. The ε values observed at physiological temperature in frequency ranges applied in such procedures are similar to ε data available for bone tissues. The observed abrupt changes in materials' behavior

due to chitosan degradation provide basis for the application of dielectric spectroscopy as nondestructive method for evaluating chitosan's stability and preservation in scaffolds (and, thus, eventual loss of important biological properties) with storage and after treatments (e.g. sterilization).

References

Ahn, P.A., Shin, E.C., Kim, G.R., & Lee, J.S. (2011). Application of generalized transmission line models to mixed ionic-electronic transport phenomena. *Journal of the Korean Ceramic Society, 48(6),* 549-558.

Barsoukov E., & Macdonald, J.R. (2005). *Impedance spectroscopy; theory, experiment, and applications*. (2nd ed.). Wiley Interscience Publications.

Baxter, F., Turner, I., Bowen, C., Gittings, J. P., & Chaudhuri, J. B. (2009). Piezoelectric hydroxyapatite composites for bone graft substitution. In *Proceedings of the UK Society for Biomaterials*, The University of Ulster, Jordanstown, Northern Ireland.

Bobritskaya, E.I., Castro, R.A., & Temnov, D. E. (2013a). Thermoactivation and dielectric spectroscopy of chitosan films. *Physics of the Solid State, 55(1),* 225–228.

Bobritskaya E., Kubrakova E., Temnov D., & Fomicheva E. (2013b). Electrical relaxation in chitosan films with mineral nanodimensional inclusions. *IZVESTIA: Herzen University Journal of Humanities and Sciences, 154,* 69-76.

Bodhak, S. (2009). *Electro-thermally polarized bulk and coated hydroxyapatite (HAp) ceramics - understanding the role of surface charge, wettability and dopants on physical, mechanical and biological properties*. Washington State University: PhD thesis.

Chakkalakal, D.A., Johnson, M.W., Harper, R.A., & Katz, J.L. (1980). Dielectric properties of fluid saturated bone. *IEEE Transactions on Biomedical Engineering, BME-27,* 95-100.

Danilchenko, S.N., Kalinkevich, O.V., Pogorelov M.V., Kalinkevich A.N., Sklyar A.M., Kalinichenko T.G., Ilyashenko V.Y., Starikov V.V., Bumeyster V.I., Sikora V.Z., & Sukhodub L.F. (2011). Characterization and in vivo evaluation of chitosan-hydroxyapatite bone scaffolds made by one step coprecipitation method. *Journal of Biomedical Materials Research Part A, 96A,* 639–647.

Kumar, D., Gittings, J.P., Turner, I.G., Bowen, C.R., Bastida-Hidalgo, A., & Cartmell, S.H. (2010). Polarization of hydroxyapatite: Influence on osteoblast cell proliferation. *Acta Biomaterialia, 6,* 1549–1554.

Dekhtyar, Y., Polyaka, N., & Sammons, R. (2008). Electrically charged hydroxyapatite enhances immobilization and proliferation of osteoblasts. *IFMBE Proceedings, 20,* 23-25.

Dutta, P. K., Dutta, J, & Tripathi V.S. (2004). Chitin and chitosan: Chemistry, properties and application. *Journal of Scientific and Industrial Research, 63,* 20-31.

Franceschetti, D.R., & Macdonald, J.R. (1979). Diffusion of neutral and charged species under small-signal A.C. conditions. Journal of Electroanalytical Chemistry, 101, 307–316.

Fu, C., Savino, K., Gabrys, P., Zeng, A., Guan, B., Olvera, D., Wang, C., Song, B., Awad, H., Gao, Y., & Yates M.Z. (2015). Hydroxyapatite thin films with giant electrical polarization. *Chemistry of Materials, 27,* 1164−1171.

Fukada, E. (1981). Piezoelectricity of bone and osteogenesis by piezoelectric films. In Becker R.O., & Thomas C.C. (Eds.), *Mechanisms of Growth Control* (pp. 192-210). Springfield, IL: Charles C. Thomas Press.

Horiuchi, N., Nakamura, M., Nagai, A., Katayama, K., & Yamashita K. (2012). Proton conduction related electrical dipole and space charge polarization in hydroxyapatite. *Journal of Applied Physics, 112,* 074901.

Horiuchi, N., Endo, J., Kosuke, N., Nakamura, M., Nagai, A., & Katayama K. (2013a). Dielectric evaluation of fluorine substituted hydroxyapatite. *Journal of Ceramic Society of Japan, 121(1417),* 770-774.

Horiuchi, N., Endo, J., Wada, N., Nozaki, K., Nakamura, M., Nagai, A., Katayama, K., & Yamashita, K. (2013b). Dielectric properties of stoichiometric and defect-induced hydroxyapatite. *Journal of Applied Physics, 113,* 134905.

Horiuchi, N., Nakaguki, S., Wada, N., Nozaki, K., Nakamura, M., Nagai, A., Katayama, K., & Yamashita K. (2014). Polarization-induced surface charges in hydroxyapatite ceramics. *Journal of Applied Physics, 116,* 014902.

Horiuchi, N., Endo, J., Wada, N., Nozaki, K., Nakamura, M., Nagai, A., Katayama, K., & Yamashita, K. (2015). Dielectric properties of fluorine substituted hydroxyapatite: the effect of the substitution on configuration of hydroxide ion chains. *Journal of Materials Chemistry B, 3,* 6790-6797.

Hoven V.P., Tangpasuthadol V., Angkitpaiboon Y., Vallapa N., & Kiatkamjornwong S. Surface-charged chitosan: Preparation and protein absorttion. (2007). *Carbohydrate Polymers, 68,* 44-53

Gittings, J.P., Bowen, C.R., Dent, A.C.E., Turner, I.G., Baxter, F.R., & Chaudhuri J.B. (2009). Electrical characterization of hydroxyapatite-based bioceramics. *Acta Biomaterialia, 5,* 743-754.

Islama, A., Imran, Z., Yasin, T., Gull, N., Khan, S.M., Shafiq, M., Sabira, A., Munawar, M.A., Raza, M.H., & Jamil T. (2015). An investigation of Ac impedance and dielectric spectroscopic properties of conducting chitosan-silane crosslinked-poly(vinyl alcohol) blended films. *Materials Research, DOI: http://dx.doi.org/10.1590/1516-1439.043715*

Itoh, S., Nakamura, S., Kobayashi, T., Shinomiya, K., & Yamashita, K. (2006). Effect of electrical polarization of hydroxyapatite ceramics on new bone formation. *Calcified Tissue International, 78,*133–142.

Itoh, S., Nakamura, S., Kobayashi, T., Shinomiya, K., Yamashita, K., & Itoh, S. (2006). Effect of electrical polarization of hydroxyapatite ceramics on new bone formation. *Calcified Tissue International, 78(3),* 133-142.

Kremer, F., Schonhals, A., & Luck, W. (2002). *Broadband dielectric spectroscopy.* Springer-Verlag.

Kumirska, J., Weinhold, M. X., Thöming, J., & Stepnowski, P. (2011). Biomedical activity of chitin/chitosan based materials - influence of physicochemical properties apart from molecular weight and degree of N-acetylation. *Polymers, 3,* 1875-1901.

Lim, C.H. (2011). Lecture 20: Warburg Impedance. In *The lecture course "Electrochemical Energy Systems"*. MIT OpenCourseWare 10.626 / 10.462.

Mascarenhas, S. (1974). The electret effect in bone and biopolymers and the bound-water problem. *Annals of New York Academy of Sciences, 238,* 36–52.

Murugaraj, P., Mainwaring, D.E., Tonkin, D.C., & Al Kobaisi M. (2011). Probing the dynamics of water in chitosan polymer films by dielectric spectroscopy. *Journal of Applied Polymer Science, 120,* 1307–1315.

Nagai, A., Yamashita, K., Imamura, M., & Azuma, H. (2008). Hydroxyapatite electret accelerates reendothelialization and attenuates intimal hyperplasia occurring after endothelial removal of the rabbit carotid artery. *Life Sciences, 82,* 1162–1168.

Nakamura, S., Kobayashi, T., Nakamura, M., & Yamashita, K. (2009). Enhanced in vivo responses of osteoblasts in electrostatically activated zones by hydroxyapatite electrets. *Journal of Materials Science: Materials in Medicine, 20,* 99–103.

Nakamura, M., Nagai, A., Hentunen, T., Salonen, J., Sekijima, Y., Okura, T., Hashimoto, K.,
Tanaka, Y., Iwasaki, T., Nakamura, M., Nagai, A., Katayama, K., & Yamashita. K. (2010). Polarization and microstructural effects of ceramic hydroxyapatite electrets. *Journal of Applied Physics, 107,* 014107.

Reedyk, C., & Perlman, M. (1968). Method for measurement of surface charge on electrets. *Journal of the Electrochemical Society, 115(1),* 49-51.

Sessler, G., & Gerhard-Multhaupt, R. (1999). *Electrets.* (4rd ed.), Morgan Hill, California: Laplacian Press.

Tarafder, S., Bodhak, S., Bandyopadhyay, A., & Bose, S. (2011). Effect of electrical polarization and composition of biphasic calcium phosphates on early stage osteoblast interactions. *Journal of Biomedical Materials Research Part B: Applied Biomaterials, 97B*, 306-314.

Telega, J.J., & Wojnar, R. (2002). Piezoelectric effects in biological tissues. *Journal of Theoretical and Applied Mechanics, 40(3),* 723-759.

Toda, Y., Monma, H., & Yamashita, K. (2009). Surface electric fields increase osteoblast adhesion through improved wettability on hydroxyapatite electret. *Applied Materials and Interfaces, 1(10),* 2181–2189.

Tofail, S.A.M., Baldisserri, C., Haverty, D., McMonagle, J. B., & Erhart, J. (2009). Pyroelectric surface charge in hydroxyapatite ceramics. *Journal of Applied Physics, 106,* 106104 – 106104-3.

Tully-Dartez, S., Cardenas, H.E., Ping-Fai, S. (2010). Pore characteristics of chitosan scaffolds studied by electrochemical impedance spectroscopy. *Tissue Engineering Part C Methods, 16(3),* 339–345.

Wang, J.C. (1987). Realizations of generalized warburg impedance with rc ladder networks and transmission lines. *Journal of the Electrochemical Society, 134(8),* 1915-1920.

Wang, Y., Qu, Y., Gong, P., Wang, P., Man, Y., & Li, J. (2010). Preparation and in vitro evaluation of chitosan bioelectret membranes for guided bone regeneration. *Journal of Bioactive and Compatible Polymers, 25(6),* 622-633.

Wang, Y., Shi, R., Gong, P., Li, J., Li, J., A, D., Wang, P., Yang, Y., Man, Y., & Qu, Y. (2012). Bioelectric effect of a chitosan bioelectret membrane on bone regeneration in rabbit cranial defects. *Journal of Bioactive and Compatible Polymers, 27(2),* 122-132.

Warburg, E. (1899). Uber das Verhalten sogenannter Unpolarisierbarer Electroden gegen Wechselstrom. *Annalen der Physik und Chemie, 67,* 493–499.

Wu, G., Gao. H., & Ma. J. (2012). Chitosan-based biomaterials. *Material Matters, 7,* n3.

Yamaguchi, I., Tokuchi, K., Fukuzaki, H., Koyama, Y., Takakuda, K., Monma, H., & Tanaka, J. (2001). Preparation and microstructure analysis of chitosan/hydroxyapatite nanocomposites. *Journal of Biomedical Materials Research, 55,* 20-27.

Yovcheva, T. A. (2010). Corona treatment of polymer films. In Bertrand C.L. (Ed.), *Electrostatics theory and applications* (p. 29). Nova Science Publishers, Inc.

Zakharov, N.A., & Orlovskii. V.P. (2001). Dielectric characteristics of biocompatible hydroxyapatite ceramics. *Technical Physics Letters, 27(8),* 629-631.

Zhao, K.S., Asami, K., & Lei J.P. (2002). Dielectric analysis of chitosan microsphere suspensions: study on its ion adsorption. *Colloid and Polymer Science, 280,* 1038–1044.

Fig. 1. Chitosan-HA nanocomposite without Ag covering (6g/L and 10g/L chitosan solution)

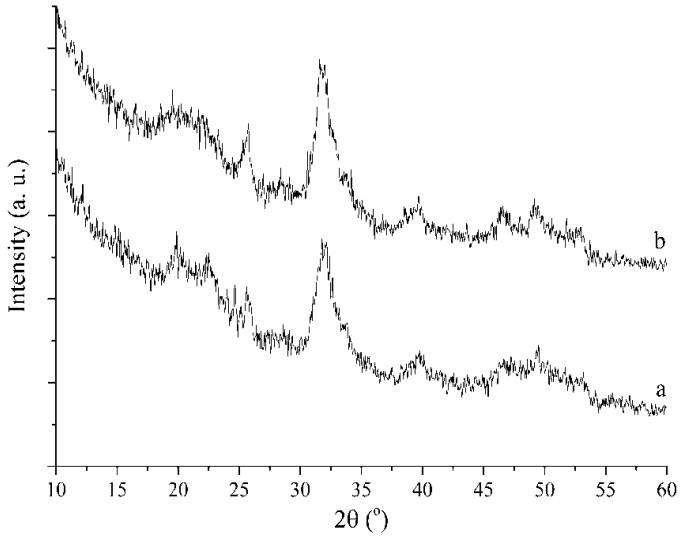

Fig. 2. XRD patterns of the synthesized composites, (a) 6 g/L, (b) 10 g/L.

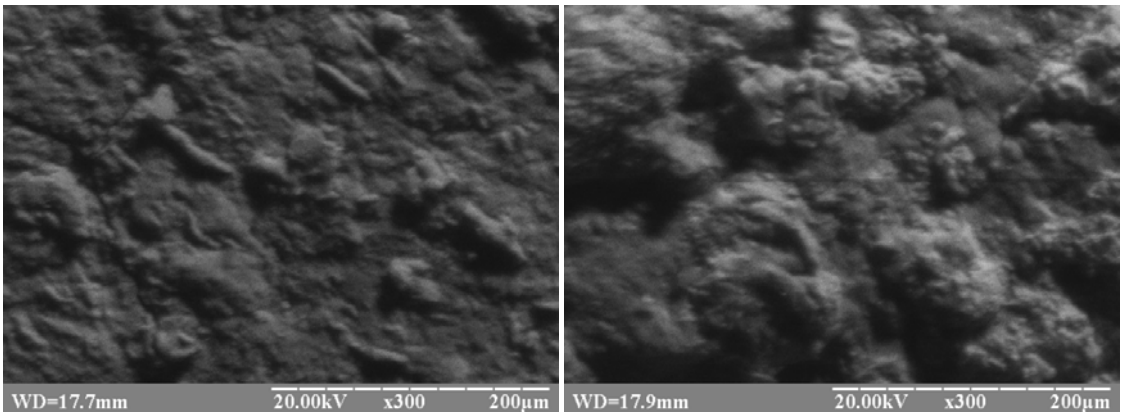

Fig. 3. SEM images (x300) of the surface of 6 g/L composite (left) and 10 g/L composite (right).

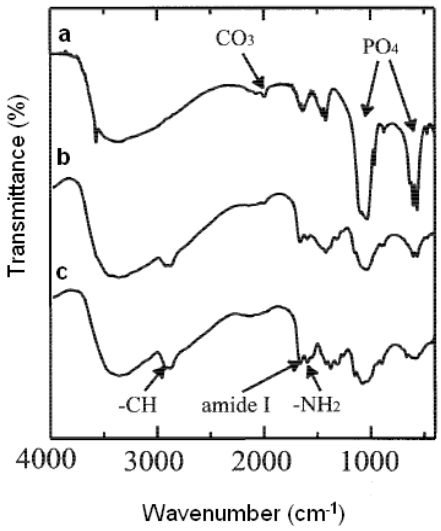

Fig. 4. IR spectrum of pure hydroxyapatite (a), 50/50 chitosan-hydroxyapatite composite (b) and pure chitosan (c).

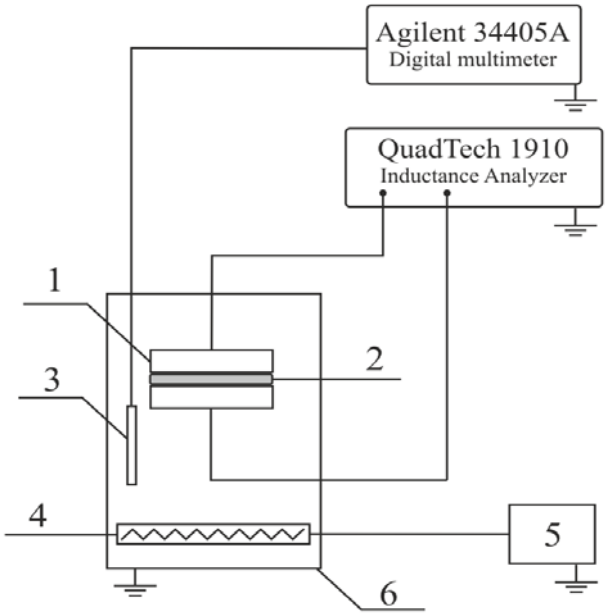

Fig. 5. Dielectric spectroscopy setup: 1 - two parallel flat electrodes; 2 - studied sample; 3 - temperature sensor; 4 - heater; 5 - power source; 6 - thermoisolated chamber

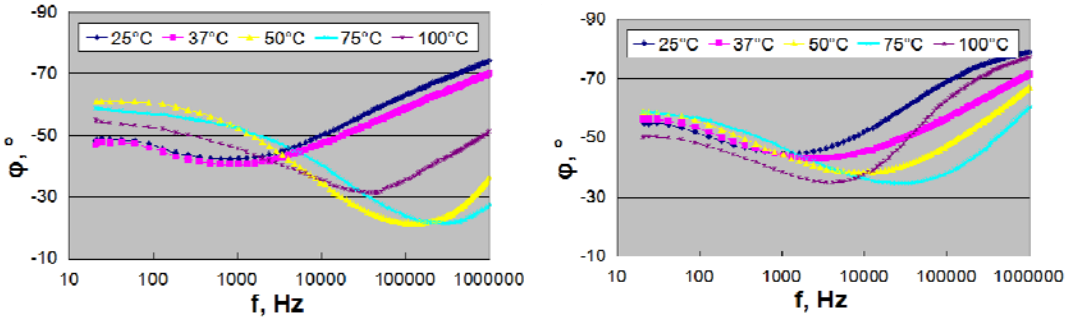

Fig. 6. Bode plots *φ(f)* at different temperatures for chitosan-HAp 50/50, prepared with 10g/l (left) and 6g/l (right) chitosan solution.

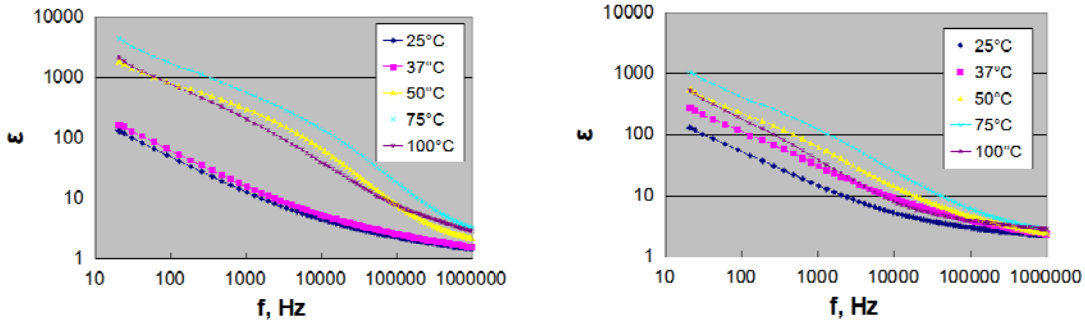

Fig. 7. Frequency dependence of the dielectric permittivity *ε(f)* at different temperatures for chitosan-HAp 50/50, prepared with 10g/l (left) and 6g/l (right) chitosan solution.

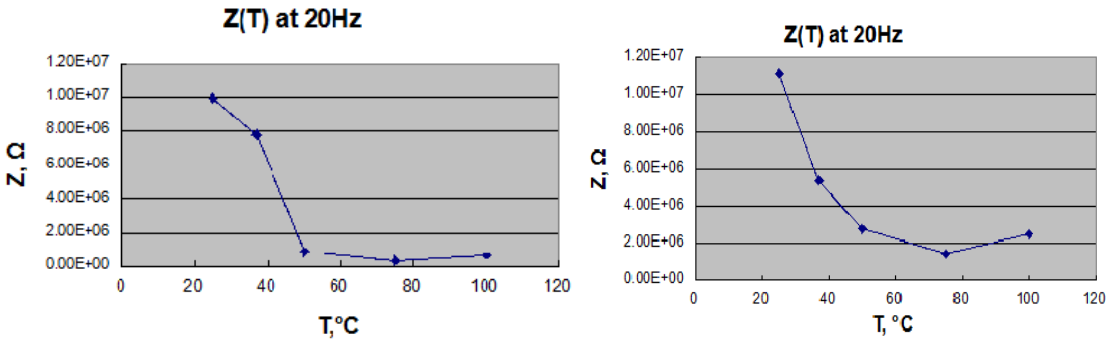

Fig. 8. Temperature dependence of the impedance modulus $|Z|(T)$ at low frequency (20Hz) for chitosan-HA 50/50, prepared with 10g/l chitosan solution (left) and 6g/l chitosan solution (right).

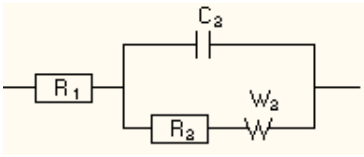

(a)

param.	sel.	sign	value	unit
R1	☐	+/-	10e3	Ohm
C2	☑	+/-	0.01 3e-9	F
R2	☑	+/-	1e3	Ohm
s2	☑	+/-	47.51e6	Ohm.s^-1/2

(b)

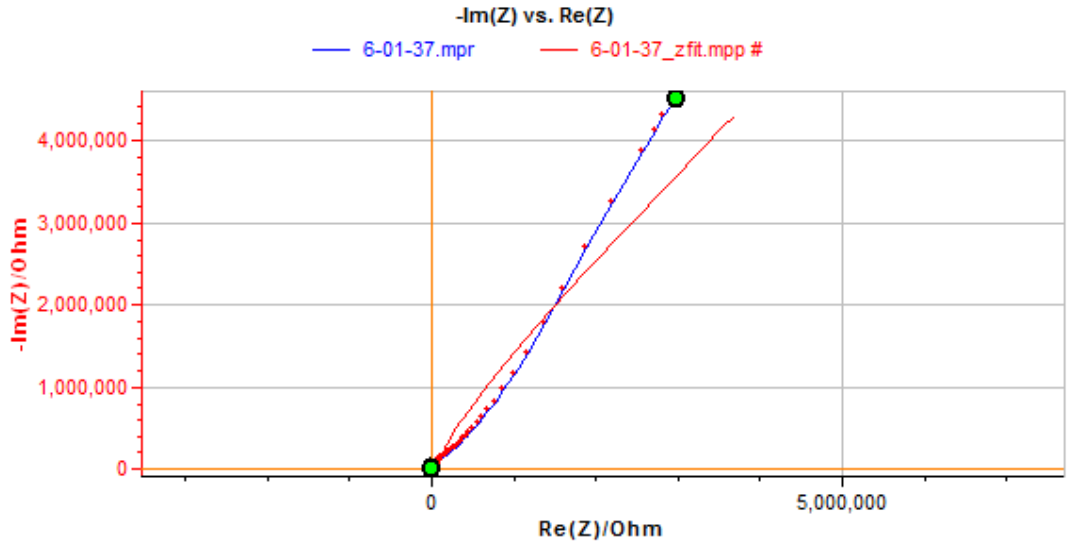

(c)

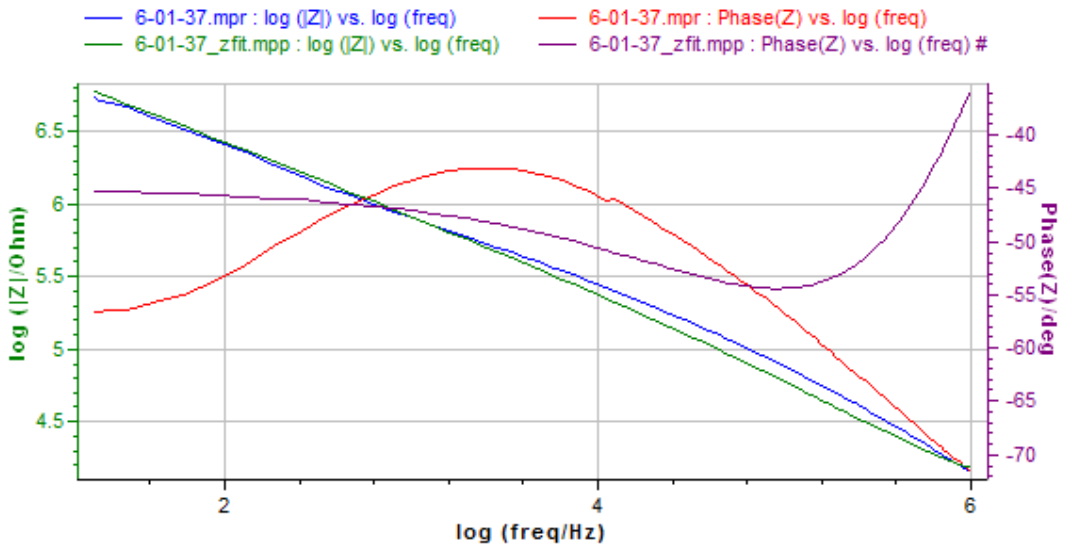

(d)

Fig. 9. Model 1: Randle's modified circuit: (a) equivalent circuit; (b) circuit parameters; (c) Nyquist plots of experimental data and simulated model circuit; (d) Bode plots of experimental data and simulated model circuit.

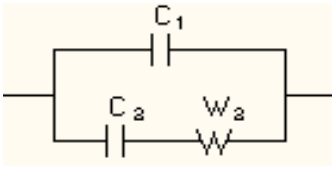

(a)

param.	sel.	sign	value	unit
C1	☑	+/-	8.987e-12	F
C2	☑	+/-	3.462e-9	F
s2	☑	+/-	31.51e-9	F.s^(1/2)

(b)

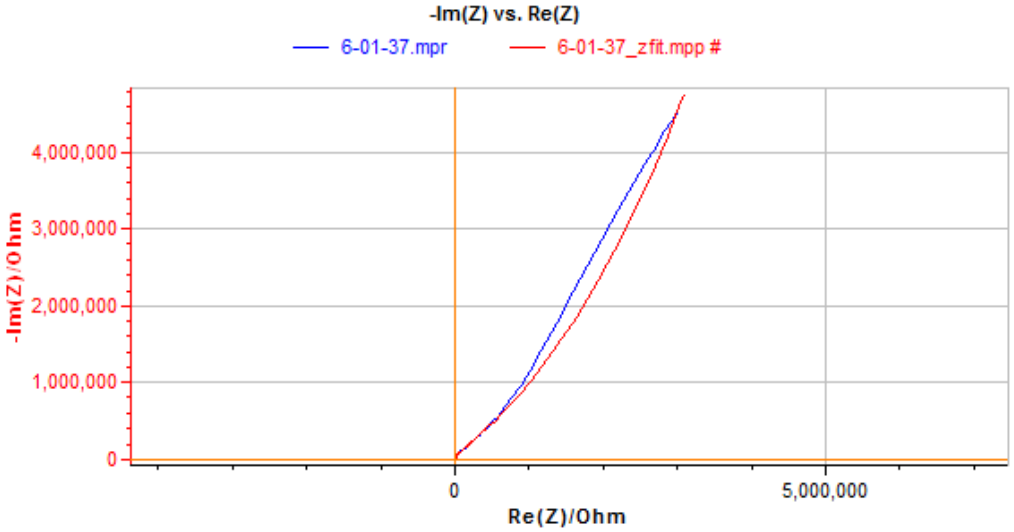

(c)

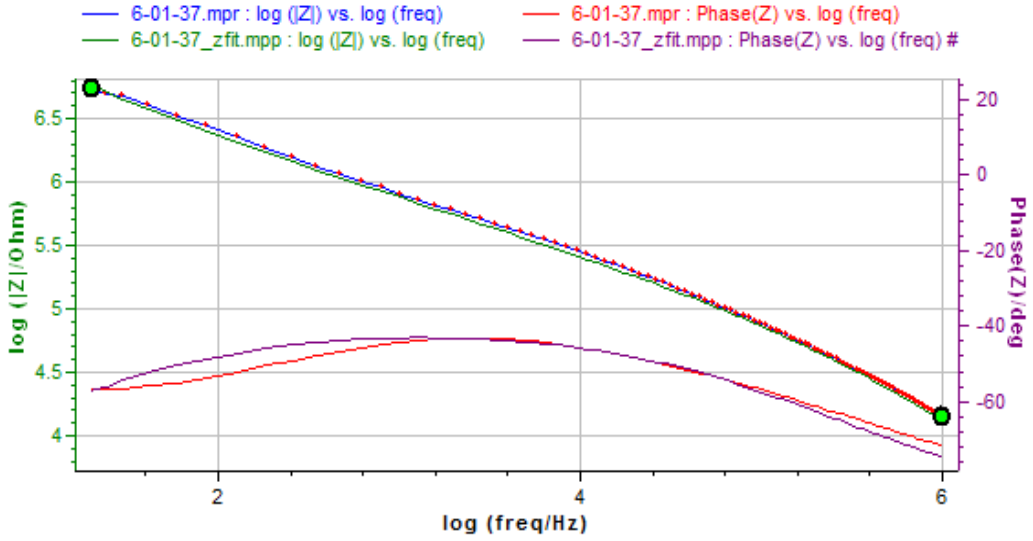

(d)

Fig. 10. Model 2: (a) equivalent circuit; (b) circuit parameters; (c) Nyquist plots of experimental data and simulated model circuit; (d) Bode plots of experimental data and simulated model circuit.

Table 1. Dielectric permittivity, ε observed at different temperatures and different frequencies

Temperature	**dielectric permittivity ε, observed at different temperatures and different frequencies**							
	chitosan-HA 50/50, prepared with 10g/l chitosan solution				chitosan-HA 50/50, prepared with 6g/l chitosan solution			
	f = 1kHz	**f = 10kHz**	**f = 100kHz**	**f = 1MHz**	**f = 1kHz**	**f = 10kHz**	**f = 100kHz**	**f = 1MHz**
25°	12,7	4,5	2,3	1,5	14,5	5,1	3,0	2,3
37°	15,8	5,3	2,6	1,6	30,6	9,0	4,0	2,4
50°	301,8	67,0	7,9	2,2	61,9	13,4	4,6	2,6
75°	560,5	140,1	18,5	3,3	119,2	24,0	6,1	2,8
100°	202,5	40,2	7,8	2,8	38,6	7,8	3,9	2,8